

## Article

# Performance Improvement of a Solar-Assisted Absorption Cooling System Integrated with Latent Heat Thermal Energy Storage

Lana Migla, Raimonds Bogdanovics  and Kristina Lebedeva \* 

Department of Heat Engineering and Technology, Riga Technical University, Kipsalas Street 6A, LV-1048 Riga, Latvia; lana.migla@rtu.lv (L.M.); raimonds.bogdanovics@rtu.lv (R.B.)

\* Correspondence: kristina.lebedeva@rtu.lv

**Abstract:** Phase change materials (PCMs) have emerged as promising solutions for latent heat thermal energy storage (LHTES) systems, offering considerable potential for storing energy derived from renewable sources across various engineering applications. The present study focused on optimization of solar cooling system by integrating LHTES with different PCM tank configurations. TRNSYS simulation software was selected for the study, and the collected experimental data from laboratory system prototype were used for system validation. The results indicate that the use of PCM led to a noteworthy decrease of 6.2% in auxiliary energy consumption. Furthermore, the time during which the heat carrier temperature flow exceeded 90 °C from the storage tank to the auxiliary fluid heater was extended by 27.8% when PCM was utilized compared to that of its absence. The use of PCM in LHTES is more effective under variable weather conditions. On the day when changes in weather conditions were observed, around 98% of the cooling load was provided by produced sun energy. The results of the research can be used to optimize the solar cooling system, which will help reduce the environmental impact of cooling systems running on non-renewable fuels.

**Keywords:** LHTES; PCM; solar energy; solar cooling system



**Citation:** Migla, L.; Bogdanovics, R.; Lebedeva, K. Performance Improvement of a Solar-Assisted Absorption Cooling System Integrated with Latent Heat Thermal Energy Storage. *Energies* **2023**, *16*, 5307. <https://doi.org/10.3390/en16145307>

Academic Editors: Ali Ashraf, Roxana Bujack and Rajib Mahamud

Received: 6 June 2023  
Revised: 29 June 2023  
Accepted: 7 July 2023  
Published: 11 July 2023



**Copyright:** © 2023 by the authors. Licensee MDPI, Basel, Switzerland. This article is an open access article distributed under the terms and conditions of the Creative Commons Attribution (CC BY) license (<https://creativecommons.org/licenses/by/4.0/>).

## 1. Introduction

Heating and cooling demands in the European Union (EU) in 2020 accounted for 50% of the total gross final energy consumption [1]. The energy efficiency of a building is primarily influenced by two key components: the building envelope and the air-conditioning system [2]. The increase in cooling degree day value from 37 in 1979 to 100 in 2021 suggests that the demand for cooling, particularly air conditioning, has indeed increased in EU over the past few decades [3]. Heatwaves are becoming more frequent and intense, particularly in southern and central European countries where the temperature reached record-high 40 °C in recent summertime [4]. The use of air conditioners and electric fans for cooling purposes account for a significant portion of electricity consumption in buildings worldwide. According to International Energy Agency (IEA) reports, cooling-related energy consumption in buildings can contribute to approximately 20% of total electricity usage [5]. Presently, ensuring a satisfactory degree of thermal comfort and minimizing the energy usage of the building has become a contentious and pressing undertaking [6]. The energy demand for cooling in the EU is continuously increasing because an inappropriate indoor climate can cause observable problems for people, which are mainly related to reduced productivity and negative health impacts [7]. This high level of energy consumption for cooling is one of today's biggest challenges due to environmental, economic, social and security factors, which means that there is an extremely urgent need to find smart, sustainable, and inclusive cooling system technologies for the EU to be climate neutral by 2050. According to a European Environment Agency (EEA) report [8], cooling technologies are mostly powered by fossil fuels.

In recent years, there has been a growing interest in cooling absorption systems due to policies aimed at reducing CO<sub>2</sub> emissions. Absorption systems, particularly those equipped

with absorption chillers for cooling applications, can indeed play a significant role in working towards climate neutrality due to their low electricity consumption making them more energy efficient compared to traditional vapor compression systems [9]. The H<sub>2</sub>O/LiBr absorption system is notable for its use of water as the coolant, which offers an environmentally friendly advantage [10]. Additionally, the heat source for the H<sub>2</sub>O/LiBr absorption system can be solar-heated water, further enhancing its environmental benefits. At present, ensuring energy independence by using renewable energy sources (RES) and improving energy efficiency has emerged as a critical subject demanding immediate attention and focused efforts [11]. Solar energy is considered one of the cleanest and most abundant energy sources available worldwide. However, one limitation of solar energy is its intermittent nature. This intermittency can pose challenges for continuous and consistent energy supply. To overcome this limitation and ensure continuous operation of the load, energy storage technologies are used. Storage for solar electricity is already a well-developed technology that has been widely used, while thermal energy storage for solar heat is currently undergoing research and development, suggesting that it has not yet reached a mature stage [12]. The integration of thermal energy storage (TES) in energy supply systems produces significant benefits in terms of system self-consumption and self-sufficiency indices [13,14]. The existing body of literature regarding TES can be categorized according to the type of heat stored, such as sensible heat storage or latent heat storage (LHS) [15]. Phase change materials (PCMs) are regarded as promising energy-saving materials due to their ability to store and release significant amounts of latent heat during isothermal phase transitions. This quality makes them suitable for delivering efficient heating or cooling energy [16,17]. The use of PCM in latent heat thermal energy storage (LHTES) enables high energy storage density while maintaining a relatively stable operating temperature [18,19]. LHTES technology holds significant value in various renewable energy applications, including electricity “peak shaving” and promoting energy efficiency in industrial and civil buildings, among other areas [20,21]. The LHTES integration into the existing solar cooling system can reduce the energy consumption and increase the system coefficient of performance (COP) [22,23]

The study is based on previous studies [24–27], and the main aim of this work is to improve the efficiency of latent heat thermal energy storage (LHTES) by proposing the different PCM tank configurations. Different types of phase change materials were selected and tested to determine their suitability for solar absorption cooling systems. In these studies, comprehensive assessment was conducted to review the selection, methodologies, integration, improvements, and challenges associated with suitable phase change materials (PCM) for operating temperatures of each component. Furthermore, the impact of PCM on the performance of a solar cooling system was calculated. Several types of phase change materials were evaluated based on various criteria, including high latent heat of fusion, conductivity, specific heat, cyclic stability, density, phase transition volume change, vapor pressure at operating temperature, melting consistency, fully reversible cycle, chemical stability, compatibility with encapsulating materials, non-corrosiveness, non-toxicity, non-explosiveness, non-flammability, environmental friendliness, cost effectiveness, and commercial availability for large-scale implementation. To enhance PCM melting, different designs for PCM containers were developed. Cylindrical geometries are known to exhibit high efficiency as storage systems, and the use of cylindrical containers with minimal dimensions further contributes to their superior performance. A study was conducted to compare heat transfer improvements among three different modifications: cylindrical form without fins, cylindrical form with circular fins, and cylindrical form with longitudinal fins. The findings suggest that the utilization of a heat transfer mechanism slightly increases the charge/discharge energy. The quantity of energy charged or discharged depends on the effectiveness of the heat transfer technique employed in the PCM modules. Based on the results obtained from these studies, paraffin RT90HC was selected as the PCM, and, consequently, cylindrical containers were chosen for the study. The research was based on a dynamic simulation of a system in TRNSYS 18 software [28]. The paper is

organized as follows: first, the Materials and Methods section starts with the description of the system and system model is presented. Second, the Results section presents the 10-day model simulation results in TRNSYS. Third, the Conclusions section is based on the results obtained from simulations.

## 2. Materials and Methods

### 2.1. Description of the System and System Model

In order to investigate the effect of PCM on the temperature stability of the tank, which is particularly important for the operation of the absorption cooling system, a model was developed in TRNSYS and validated with the real system. The research focuses on optimizing energy storage by integrating containers with phase change materials, which can decrease the consumption of auxiliary fluid heater energy and increase the coefficient of performance (COP) of the solar cooling system. The study also aims to reduce the environmental impact of the cooling system. The system studied in this research consists of vacuum solar collectors (SC) connected via heat exchanger to a 1 m<sup>3</sup> heat storage tank containing PCM in the top part of the tank (see Figure 1). The system utilizes water from the tank as a heat source for an absorption chiller with a cooling tower (CT). In cases where the water temperature is insufficiently high, an auxiliary electric heater is used to raise the temperature of the water before chiller.

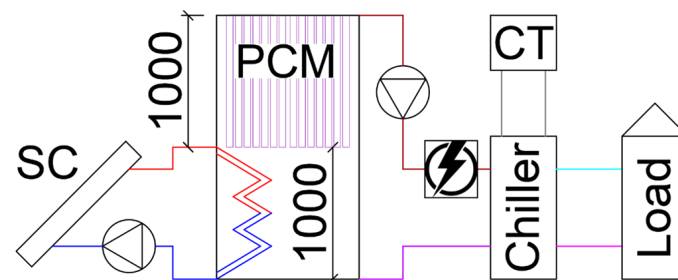


**Figure 1.** Principle drawing of the studied system.

The research was based on a dynamic simulation of a system (see Figure 2). The system model was created using the TRNSYS 18 software (version 18.04.0001), and various scenarios were explored by varying the amount of phase change materials in the tank, the number of installed vacuum solar collectors, the cooling loads and auxiliary fluid heater temperature setpoint.

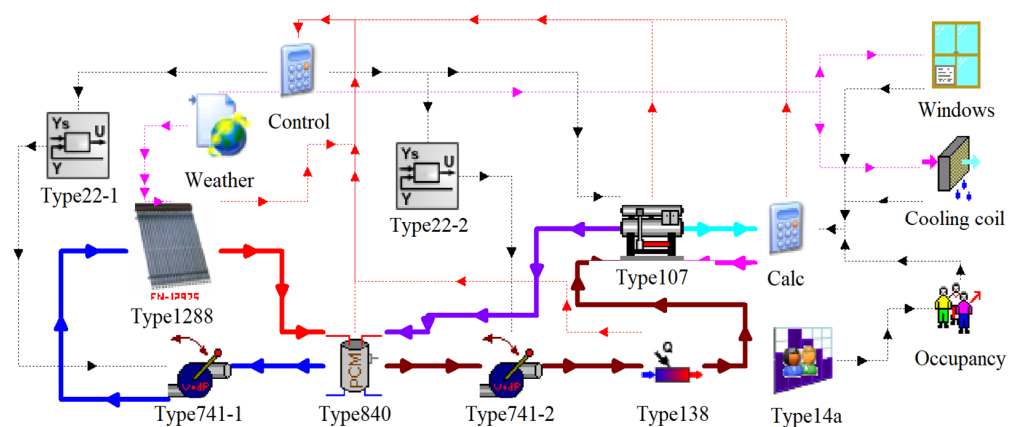


**Figure 2.** TRNSYS 18 model of Solar Cooling system with PCM thermal energy storage.

For a detailed description of the system elements, see Table 1.

**Table 1.** Main Type descriptions used for simulation.

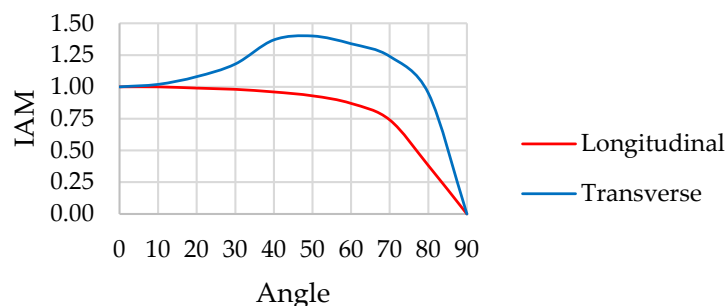
Types	Description	Parameters
Type 1288	Vacuum solar collector	Area (total) = 28 m <sup>2</sup> Efficiency = 0.568 $\alpha_1 = 1.04 \text{ W/m}^2\text{K}$ $\alpha_2 = 0.0024 \text{ W/m}^2\text{K}^2$ Heat capacity = 6.5 kJ/m <sup>2</sup> K Volume 1000 L Height 2 m
Type 840	PCM tank	Insulation 100 mm mineral wool Water specific heat capacity 4.2 kJ/kgK Density 970 kg/m <sup>3</sup> Effective vertical thermal conductivity 2 W/mK
Type 741-1 Type 741-2	Circulation pump	Efficiency 0.6 Motor efficiency 0.9 Pressure drop 50 kPa
Type 138 Type 107	Auxiliary Fluid Heater Absorption Chiller	Efficiency 100% (electrical heater) COP 0.5 to 0.8
Type 687	Windows	Solar heat gain from windows: total area 12 m <sup>2</sup> , solar heat gain coefficient 0.6, vertical surface facing south
Type 574	Occupancy	Activity level—seated, light work, typing
Type 752	Air cooling coil	With dry air flowrate 300 kg/h and temperature setpoint 18 °C

All the types used for simulation with their main used parameters are described right after Figure 2 in Section 2.2 in the text.

## 2.2. System Model Components

### 2.2.1. Vacuum Solar Collector

The following parameters were considered in the study: vacuum solar collector (Type 1288) area (total) = 28 m<sup>2</sup>; efficiency = 0.568;  $\alpha_1 = 1.04 \text{ W/m}^2\text{K}$ ;  $\alpha_2 = 0.0024 \text{ W/m}^2\text{K}^2$ ; heat capacity = 6.5 kJ/m<sup>2</sup>K, IAM for diffuse radiation = 0.1 (see Figure 3). The inclination of solar collectors was at 45° to the south. At the ambient air temperature of +25 °C, mean heat carrier temperature in the collector was +90 °C, and with solar radiation on the surface of 1000 W/m<sup>2</sup>, the simulated solar plant (28 m<sup>2</sup>) may produce 13.7 kW of heating energy.

**Figure 3.** Solar collector incidence angle modifier (IAM).

### 2.2.2. PCM Tank

PCM tank (Type 840) was created by the authors of [29]. The Institute of Thermal Engineering at Graz University of Technology developed the simulation model Type 840, which allows for detailed simulations of water tanks containing integrated PCM modules of various geometries such as cylinders, spheres, and plates. Alternatively, the model can simulate tanks filled with a PCM slurry. The heat transfer within the PCM modules is calculated by considering conduction only while disregarding convection effects in the liquid phase. Transient heat conduction in the PCM modules is modeled using a

two-dimensional approach for cylinders and plates, and a one-dimensional approach for spheres, employing finite differences. The phase change process is simulated using the enthalpy method, assuming the specific enthalpy as a continuous function of temperature. The model also takes into account phenomena like supercooling and hysteresis that often occur with various PCMs. Both TRNSYS 17 and TRNSYS 18 versions of the model are available. The parameters for the designed thermal tank are as follows: volume, 1000 L; height 2 m; the tank is insulated with a 100 mm mineral wool, the total heat loss rate is determined by formula ( $2.26 \times \Delta T + 0.0072 \times \Delta T^2$ ), where  $\Delta T$  is the temperature difference between average tank temperature and outside air temperature. Water specific heat capacity is 4.2 kJ/kgK and density is 970 kg/m<sup>3</sup>; effective vertical thermal conductivity is 2 W/mK.

The following are the PCM tank properties: outer diameter, 54 mm; thickness, 1.5 mm; length, 1 m; thermal conductivity, 395 W/mK; specific heat capacity, 0.38 kJ/kgK; density, 8900 kg/m<sup>3</sup>.

Based on the material properties and average cost, it was decided to use commercially available material RT90HC. The following are the PCM properties: specific heat capacity, 2 kJ/kgK; phase change enthalpy, 170 kJ/kg; temperature at the start of phase change, 91 °C; temperature at the end of phase change, 92 °C; temperature difference (hysteresis) between the melting and solidification curves, 1 °C; density of the PCM material, 850 kg/m<sup>3</sup>; thermal conductivity material, 0.2 W/mK.

It is geometrically possible to install 154 PCM containers (see Figure 4), which results in 35.3% of volume of the tank. Additionally, cases with 52 (11.9%), 80 (18.3%) and 114 (26.1%) PCM containers were investigated.

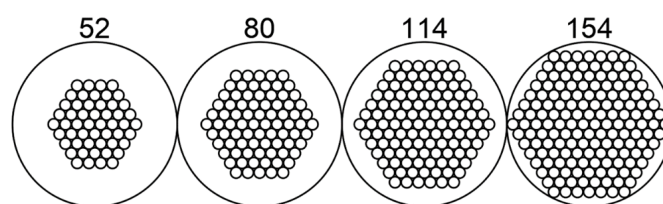


Figure 4. Phase change material possible placement in the tank, top view.

### 2.2.3. Circulation Pump

The following are the properties of the circulation pump (Type 741-1 and Type 741-2): overall pump efficiency, 0.6; motor efficiency, 0.9; pressure drop, 50 kPa; motor is mounted within the fluid stream. The circulation pump is controlled by Iterative feedback controller (Type 22-1 and Type 22-2) to provide a 5 °C heat carrier temperature difference between supply and return pipes of the solar collector loop and a 10 °C heat carrier temperature difference between supply and return pipes of the chiller loop. The pipe thermal losses and pipe capacitances were not considered, as they are not relevant to this study.

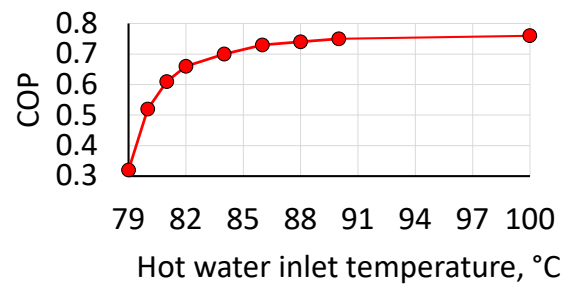
### 2.2.4. Auxiliary Fluid Heater

Auxiliary Fluid Heater (Type 138) has the efficiency of 100% (electrical heater).

### 2.2.5. Absorption Chiller

Solar energy is generated by a system of solar thermal collectors and stored in a thermal energy storage tank. The hot heat carrier from the thermal energy storage is fed to the generator to boil the water vapor from the H<sub>2</sub>O/LiBr solution. The resulting water vapor is then cooled in a condenser before being directed to an evaporator. In the evaporator, the vapor is further cooled and evaporated under lower pressure and temperature conditions. The solution leaving the generator and flowing to the absorber passes through a solution heat exchanger to preheat the weak solution stream entering the generator. In the absorber, the solution absorbs the water vapor flowing from the absorber to the evaporator. An additional heater is provided to raise the temperature of the hot water supplied; if this is not sufficient to operate the generator, the heat transfer medium is heated to the required temperature for the generator. The main advantage of absorption systems is that the amount of electricity to run

the system is limited to the solution pump, which, compared to vapor compression systems, does not consume as much electricity for compression. When comparing absorption cycle COP (0.5 to 0.8) [30] to traditional cooling systems, the absorption cycle efficiency optimization becomes significant. Regarding Hot Water-Fired Single-Effect Absorption Chiller (Type 107), COP is defined by external file according to Figure 5. Cooling tower is not presented in the model. It is assumed that the cooling water inlet temperature is 30 °C and the flowrate is 3000 kg/h. Chilled water setpoint is 7 °C.



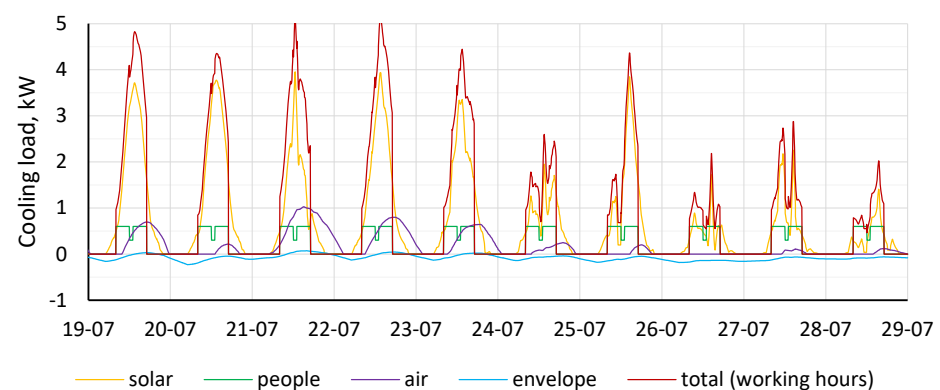
**Figure 5.** Absorption chiller coefficient of performance depending on heat source temperature. Data from [31].

Figure 5 illustrates the relationship between the hot water inlet temperature and the COP of the system. It is observed that the COP of the system increases as the water temperature rises. However, it should be noted that water–lithium bromide pair systems are unable to exceed 100 °C due to the issue of crystallization [32]. The manufacturer of the machine specifies an ideal COP range of 0.7 to 0.78. This range is supported by the simulation results for the initial conditions mentioned earlier, where the COP is determined to be 0.75 [31].

As depicted in Figure 4, the COP can reach its maximum value of 0.82 by reducing the absorber and condenser temperatures to 30 °C.

#### 2.2.6. Base Load

Base load (see Figure 6) is calculated dynamically based on the sum of the following parameters.



**Figure 6.** Base load during analyzed period.

1. Solar heat gain from windows (Type 687): total area 12 m<sup>2</sup>, solar heat gain coefficient 0.6, vertical surface facing south;
2. Occupancy (Type 574): activity level—seated, light work, typing. Schedule defined by (Type 14a): 4 people from 8:00 to 12:00, 2 people from 12:00 to 13:00 and 4 people from 13:00 to 17:00;
3. Ventilation air cooling coil (Type 752) with dry air flowrate 300 kg/h and temperature setpoint 18 °C;
4. Envelope: window loss coefficient 1.1 W/m<sup>2</sup>.

Chiller is operated by total cooling load only during working hours (8:00–17:00).

### 2.2.7. Climate Data, Simulated Period and Variables

Climate data: Meteonorm\Europe\LV-Riga.tm2.

Simulated period: 18–29 July. The simulation timestep is 60 s. The first day is not used in the analysis, as it is simulated to determine the initial conditions in the tank. In total, 5 days are sunny, 5 days are cloudy.

Variables:

- P—number of PCM modules (0/52/80/114/154);
- L—fraction of base load (0.5/1/1.5/2);
- S—area (m<sup>2</sup>) of solar collectors (12/20/28/36/44);
- T—auxiliary fluid heater temperature setpoint (°C).

## 3. Results

The results presented in this study are based on a 10-day simulation in TRNSYS. The electricity consumption of the auxiliary fluid heater was used as the primary parameter to evaluate the efficiency of the system across various scenarios.

Initially, the optimal setpoint temperature for the auxiliary fluid heater was determined. According to Figure 7, this was found to be between 83 °C and 85 °C. Operating the system with a lower setpoint resulted in a lower COP of the chiller, as shown in Figure 5. However, setting the setpoint higher led to an increase in electricity consumption due to a reduction in tank heat storage capacity and an increase in heat losses. Consequently, a setpoint of 84 °C was used for further calculations.

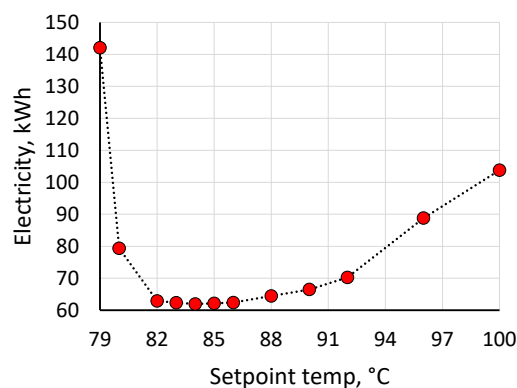


**Figure 7.** Auxiliary fluid heater energy consumption based on heating temperature setpoint during the 10-day period. P = 154; L = 1; S = 28.

The impact of solar collector area on the performance of the system was studied, as shown in Figure 8 (left), under two scenarios: one without PCM in the storage tank, and another with 154 PCM modules. When the solar collector area was small (12 m<sup>2</sup>), the use of PCM led to a 0.4% increase in electricity consumption. This can be attributed to the fact that the temperature inside the storage tank was mostly below the PCM melting temperature, resulting in a decrease in the total storage capacity due to the lower specific heat capacity of the PCM (2 kJ/kgK) compared to water (4.2 kJ/kgK). However, as the solar collector area was increased, the electricity consumption decreased and the impact of the PCM became more significant. The energy savings achieved through the use of PCM peaked at a solar collector area of 28 m<sup>2</sup>, resulting in a reduction of 6 kWh, which remained relatively stable with further increases in collector area. A solar collector area of 28 m<sup>2</sup> was used for further calculations.

The next task was to assess the effect of cooling loads on the system performance by varying the base load (Figure 5) by a factor of 0.5, 1.5, and 2. The findings are illustrated in Figure 8 (right). The use of PCM was found to have the most pronounced influence at lower cooling loads, while excessively high cooling loads resulted in a 1.0% increase in

auxiliary fluid heater electricity consumption, similarly as it happened in case with low numbers of installed solar collectors. Thus, a proper design of the number of collectors based on actual cooling load is essential to optimize system performance.

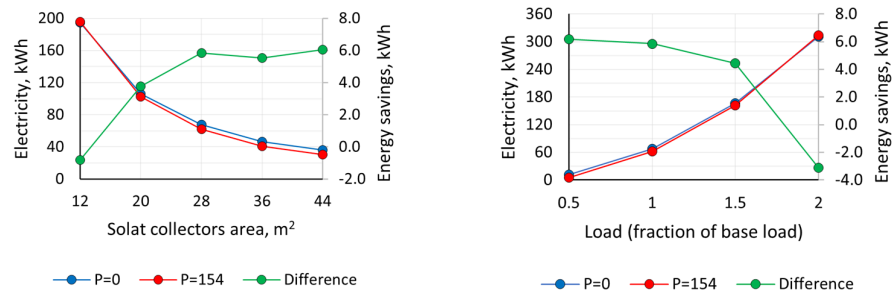


**Figure 8.** Auxiliary fluid heater energy consumption dependence on solar collector area ((left); L = 1, T = 84) and cooling load ((right); S = 28, T = 84) during the 10-day period.

The regression analysis revealed a linear relationship between the volume of PCM and electricity consumption (see Figure 9).

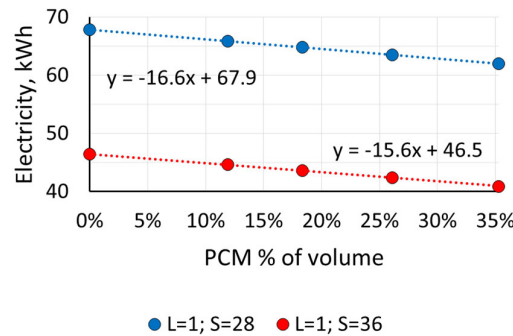


**Figure 9.** Auxiliary fluid heater energy consumption dependence on solar collector area (left; L = 1, T = 84) and cooling load (right; S = 28, T = 84) during the 10-day period.

Figure 10 illustrates the heat carrier temperature from the storage tank to the auxiliary fluid heater. During periods with sufficient solar energy (19.07–21.07), the heat carrier temperature was slightly lower in the case with PCM modules compared to the case without PCM, resulting in lower heating energy losses in the tank. The main impact of PCM was observed when the weather changed (24.07) and the total cooling load exceeded the amount of produced solar energy. This observation confirms that the PCM effect is significant under fluctuating conditions. Despite this, the heat carrier temperature remained above 90 °C for a longer period of time, resulting in lower electricity usage by the auxiliary fluid heater, as shown in Table 2.

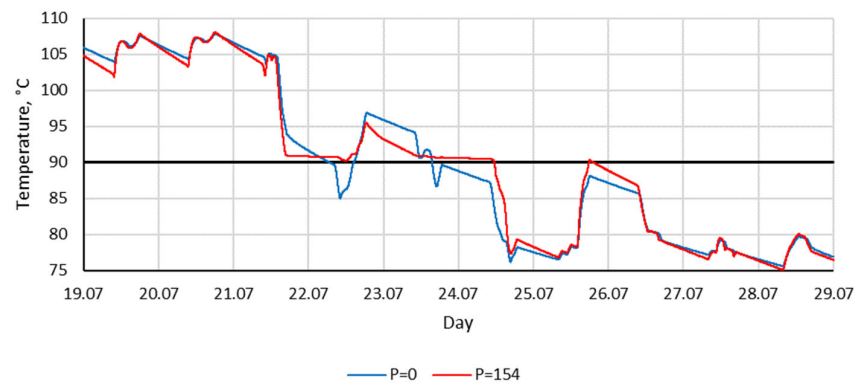


**Figure 10.** Heat carrier temperature from PCM tank to chiller (before auxiliary fluid heater) during 10-day period. S = 28, L = 1, T = 84.

**Table 2.** TRNSYS simulation results for cases with S = 28, L = 1, T = 84.

Period	Produced Solar Energy, kWh		Cooling Load, kWh		Auxiliary Fluid Heater el. Consumption, kWh		Storage Tank Heat Loss, kWh	
	P = 0	P = 154	P = 0	P = 154	P = 0	P = 154	P = 0	P = 154
19.07	65.92	65.95	30.27	30.27	0.00	0.00	−5.86	−5.80
20.07	65.12	65.13	27.25	27.25	0.00	0.00	−5.89	−5.86
21.07	23.98	24.35	28.83	28.83	0.00	0.00	−5.31	−5.21
22.07	54.11	53.47	30.19	30.19	0.00	0.00	−4.60	−4.57
23.07	31.53	31.35	26.15	26.15	0.00	0.00	−4.71	−4.64
24.07	3.34	3.29	14.74	14.74	8.66	3.37	−4.03	−4.18
25.07	25.89	25.59	19.66	19.66	16.54	15.26	−3.92	−3.99
26.07	0.00	0.00	9.04	9.04	7.01	7.51	−4.03	−4.07
27.07	3.44	3.42	14.20	14.20	18.64	19.10	−3.68	−3.67
28.07	0.00	0.00	9.14	9.14	16.96	16.74	−3.67	−3.66
Total	273.32	272.55	209.49	209.49	67.82	61.96	−45.70	−45.66

Figure 11 shows the temperature profile inside the storage tank with a 0.5 m vertical step, where 1 represents the top and 5 represents the bottom of the tank.

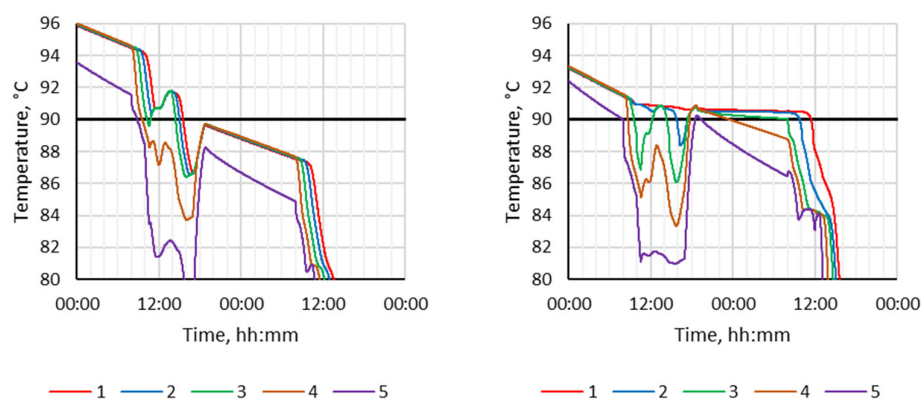


**Figure 11.** Tank temperature at different height. From 23.07 00:00 to 24.07 24:00. P = 0 (left), P = 154 (right). S = 28, L = 1, T = 84.

#### 4. Discussion

Additionally, to analyze the performance of solar cooling systems in summer season, two simulation cases (P0, L1, S28, T84 and P154, L1, S28, T84) were evaluated for the period between 31.05 and 31.08, with the initial conditions in the tank determined from a simulation of 31.05 (which was excluded from the analysis). During the summer months, the TRNSYS simulation results indicate that 2766 kWh of solar energy was produced, out of which 14.7% was lost as heat from the storage tank. The cooling load was 1945 kWh, and the electricity consumption of the two circulation pumps was 18 kWh. The auxiliary fluid heater electricity consumption was 776 kWh without PCM, while it was 727 kWh with 154 PCM modules. The use of PCM resulted in a 6.2% reduction in auxiliary energy consumption. Moreover, the period of time with heat carrier temperature flow from the storage tank to the auxiliary fluid heater exceeding 90 °C was 27.8% longer with the use of PCM in comparison to that without it.

The utilization of PCM yielded the highest energy savings when the solar collector area reached 28 m<sup>2</sup>, resulting in a reduction of 6 kWh. This energy-saving benefit remained relatively consistent, even with further increases in the collector area.

This work is dedicated only to the design of possible LHTES construction for solar cooling system optimization. The economic issues of the system are outside of the scope of this work, although studies show that some LHTES not only increase the efficiency of the system, but also have a relatively low cost [33,34]. The main drawback of this work

is the inability to determine the profitability of the proposed system at the moment, as only a system prototype was developed for the time being. However, this aspect will be considered in our next work, when the system prototype will be tested in real conditions.

## 5. Conclusions

The developed LHTES construction for solar cooling system was successfully validated in laboratory conditions through experimental data collected during a measurement analysis carried out at the Riga Technical University (RTU) in the framework of project “Latent heat storage for sustainable cooling”.

This paper presents and examines the simulation outcomes achieved by this model across different LHTES PCM tank construction—PCM placement in the tank, providing detailed analysis and discussion of the findings. The results are used to optimize the operation of the solar cooling system by integrating LHTES into it. More specifically, the considered solar cooling system with LHTES is simulated for air conditioning for the needs of a small office in Latvia, Riga using experimental data from the solar cooling system laboratory prototype developed by RTU.

As a result of the research, it is concluded that such design LHTES optimization approach (the main effect of PCM) is observed when the weather changes, and the total cooling load exceeds the amount of solar energy produced. The aim of the paper is achieved, namely to determine the impact of LHTES on the performance of an absorption solar cooling system. By studying specific days with different weather conditions in depth, it is determined that the greatest positive impact of the PCM containers is directly under changing weather conditions, when sunny days alternate with cloudy days, which is particularly characteristic of Latvian climatic conditions. A reduction in auxiliary energy consumption is found, which has a positive impact on the EU’s climate neutrality ambition.

Closer examination of two types of thermal energy storages—Sensible (without PCM) and Latent (with 154 containers with PCM)—shows that under changing weather conditions (alternating sunny and cloudy days, see Figure 10), the LTHS efficiency and positive impact on the overall system COP increases significantly.

A thorough investigation is conducted on the variances associated with different PCM fill ratios. The maximum fill ratio observed is 35.3% of the tank volume, which equates to 154 PCM containers. However, it is determined that using less PCM than the maximum does not significantly impact the tank temperature and, consequently, the overall system performance. It is concluded that finding a balance between costs and efficiency gains is crucial.

It is found that when the solar collector area is limited to 12 m<sup>2</sup>, the integration of PCM results in a marginal 0.4% increase in electricity consumption. This can be attributed to the fact that the temperature inside the storage tank remains predominantly below the melting temperature of the PCM. However, as the solar collector area is expanded, the electricity consumption progressively decreases, and the influence of the PCM becomes more pronounced.

Changes in weather conditions for Latvia’s climate are common due to the influence of the Baltic Sea, which only proves that the proposed LHTES optimization approach can be useful and effective. It is observed that the beneficial effect of PCMs on the efficiency of LHTES occurs on days with variable weather conditions or fluctuating solar energy availability. The effect is less pronounced under prolonged sunny conditions as the temperature in the tank does not fluctuate but remains constant. The studied LHTES solution can be used not only in solar assisted absorption cooling systems, but also when the heat source is wasting heat from various processes.

**Author Contributions:** Conceptualization, L.M. and K.L.; methodology, L.M.; software, R.B.; validation L.M. and R.B.; formal analysis, K.L.; investigation, L.M., R.B. and K.L.; data curation, L.M.; writing—original draft preparation, L.M.; writing—review and editing, L.M. and K.L.; visualization, R.B. All authors have read and agreed to the published version of the manuscript.

**Funding:** This work has been supported by the European Regional Development Fund within the Activity 1.1.1.2 “Post-doctoral Research Aid” of the Specific Aid Objective 1.1.1 “To increase the research and innovative capacity of scientific institutions of Latvia and the ability to attract external financing, investing in human resources and infrastructure” of the Operational Programme “Growth and Employment” (No.1.1.1.2/VIAA/4/20/661).

**Data Availability Statement:** Not applicable.

**Conflicts of Interest:** The authors declare no conflict of interest.

## References

1. Eurostat. Additional Data—Energy—Eurostat. Available online: <https://ec.europa.eu/eurostat/web/energy/database/additional-data> (accessed on 31 May 2023).
2. Borodinecs, A.; Gaujens, B. The implementation of building envelopes with controlled thermal resistance. In Proceedings of the 10th International Conference on Healthy Buildings 2012, Brisbane, Australia, 8–12 July 2012; International Society of Indoor Air Quality and Climate (ISIAQ): Brisbane, Australia, 2012; pp. 1715–1722. Available online: [https://alephfiles.rtu.lv/TUA01/000039268\\_e.pdf](https://alephfiles.rtu.lv/TUA01/000039268_e.pdf) (accessed on 31 May 2023).
3. Eurostat. Heating of Buildings Decreasing, Cooling Increasing—Products Eurostat News—Eurostat. Available online: <https://ec.europa.eu/eurostat/en/web/products-eurostat-news/-/ddn-20220531-1> (accessed on 31 May 2023).
4. Energy Monitor. Cooling Europe: Urgent but Not Yet Low-Carbon. Available online: <https://www.energymonitor.ai/sectors/heating-cooling/europe-what-about-cooling/> (accessed on 31 May 2023).
5. IEA. The Future of Cooling—Analysis—IEA. Available online: <https://www.iea.org/reports/the-future-of-cooling> (accessed on 31 May 2023).
6. Deshko, V.; Buyak, N.; Bilous, I.; Voloshchuk, V. Reference state and exergy based dynamics analysis of energy performance of the ‘heat source—Human—Building envelope’ system. *Energy* **2020**, *200*, 117534. [CrossRef]
7. Staveckis, A.; Borodinecs, A. Impact of impinging jet ventilation on thermal comfort and indoor air quality in office buildings. *Energy Build.* **2021**, *235*, 110738. [CrossRef]
8. European Environment Agency’s Home Page. Available online: <https://www.eea.europa.eu/en> (accessed on 31 May 2023).
9. Zheng, J.; Castro, J.; Oliva, A.; Oliet, C. Energy and exergy analysis of an absorption system with working pairs LiBr-H<sub>2</sub>O and Carrol-H<sub>2</sub>O at applications of cooling and heating. *Int. J. Refrig.* **2021**, *132*, 156–171. [CrossRef]
10. Blanco-Marigorta, A.M.; Marcos, J.D. Key issues on the exergetic analysis of H<sub>2</sub>O/LiBr absorption cooling systems. *Case Stud. Therm. Eng.* **2021**, *28*, 101568. [CrossRef]
11. Krizmane, M.; Slihte, S.; Borodinecs, A. Key Criteria Across Existing Sustainable Building Rating Tools. *Energy Procedia* **2016**, *96*, 94–99. [CrossRef]
12. Kwasi-Effah, C.C.; Ighodaro, O.; Egbare, H.O.; Obanor, A.I. A novel empirical model for predicting the heat accumulation of a thermal energy storage medium for solar thermal applications. *J. Energy Storage* **2022**, *56*, 105969. [CrossRef]
13. Tola, V.; Arena, S.; Cascetta, M.; Cau, G. Numerical investigation on a packed-bed LHTES system integrated into a micro electrical and thermal grid. *Energies* **2020**, *13*, 2018. [CrossRef]
14. Rusovs, D.; Jaundalders, S.; Stanka, P. Pumped thermal electricity storage integration in district heating systems. In Proceedings of the 2020 IEEE 61st Annual International Scientific Conference on Power and Electrical Engineering of Riga Technical University, RTUCON 2020—Proceedings, Riga, Latvia, 5–7 November 2020. [CrossRef]
15. Raut, D.; Kalamkar, V.R. A review on latent heat energy storage for solar thermal water-lithium bromide vapor absorption refrigeration system. *J. Energy Storage* **2022**, *55*, 105828. [CrossRef]
16. Shi, J.; Qin, M.; Aftab, W.; Zou, R. Flexible phase change materials for thermal energy storage. *Energy Storage Mater.* **2021**, *41*, 321–342. [CrossRef]
17. Szajding, A.; Kuta, M.; Cebo-Rudnicka, A.; Rywotycki, M. Analysis of work of a thermal energy storage with a phase change material (PCM) charged with electric heaters from a photovoltaic installation. *Int. Commun. Heat Mass Transf.* **2023**, *140*, 106547. [CrossRef]
18. Niu, F.; Ni, L.; Yao, Y.; Yu, Y.; Li, H. Performance and thermal charging/discharging features of a phase change material assisted heat pump system in heating mode. *Appl. Therm. Eng.* **2013**, *58*, 536–541. [CrossRef]
19. Anita, A.N.; Ramachandran, S. Design analysis of heat exchanger for the solar water heating systems using phase change materials. *Mater. Today Proc.* **2021**, *47*, 4533–4537. [CrossRef]
20. Li, J.; Zhang, Y.; Peng, Z.; Zhang, X.; Zhai, J.; Luo, Y.; Liu, B.; Sun, X.; Al-Saadi, S.N. Thermal performance of a plate-type latent heat thermal energy storage heat exchanger—An experimental investigation and simulation study. *J. Energy Storage* **2023**, *65*, 107295. [CrossRef]
21. Panchal, J.M.; Modi, K.V.; Patel, V.J. Development in multiple-phase change materials cascaded low-grade thermal energy storage applications: A review. *Clean Eng. Technol.* **2022**, *8*, 100465. [CrossRef]
22. Çam, N.Y.; Alptekin, E.; Bilir, L.; Ezan, M.A. Thermal behavior of a solar-assisted latent heat thermal energy storage unit on the heating season under variable weather conditions. *J. Energy Storage* **2022**, *52*, 104934. [CrossRef]

23. Qv, D.; Ni, L.; Yao, Y.; Hu, W. Reliability verification of a solar–air source heat pump system with PCM energy storage in operating strategy transition. *Renew. Energy* **2015**, *84*, 46–55. [[CrossRef](#)]
24. Snegirjovs, A.; Shipkovs, P.; Lebedeva, K.; Kashkarova, G.; Migla, L.; Gantenbein, P.; Omlin, L. Performance Evaluation of Photovoltaic Solar Air Conditioning. *Latv. J. Phys. Tech. Sci.* **2016**, *53*, 29–36. [[CrossRef](#)]
25. Lebedeva, K.; Migla, L. Latent thermal energy storage for solar driven cooling systems. *Eng. Rural Dev.* **2020**, *19*, 1134–1139. [[CrossRef](#)]
26. Migla, L.; Lebedeva, K. A Review for Phase Change Materials in Solar Cooling Systems. In Proceedings of the 2021 10th International Conference on Power Science and Engineering (ICPSE), Istanbul, Turkey, 21–23 October 2021; pp. 110–116. [[CrossRef](#)]
27. Migla, L.; Lebedeva, K. Optimization model of solar cooling system with latent heat storage. *Acta Polytech. CTU Proc.* **2022**, *38*, 295–301. [[CrossRef](#)]
28. Klein, S.A. *TRNSYS 18: A Transient System Simulation Program*. Solar Energy Laboratory; The University of Wisconsin: Madison, WI, USA, 2017; Volume 3.
29. Moser, C.; Heinz, A.; Schranzhofer, H. *TRNSYS Type 840: Simulation Model for PCM/Water Storage Tanks (Version 3.0) (V3.0)*; Graz University of Technology: Graz, Austria, 2022.
30. Eicker, U.; Pietruschka, D. Design and performance of solar powered absorption cooling systems in office buildings. *Energy Build.* **2009**, *41*, 81–91. [[CrossRef](#)]
31. Ketfi, O.; Merzouk, M.; Merzouk, N.K.; El Metenani, S. Performance of a Single Effect Solar Absorption Cooling System (Libr-H<sub>2</sub>O). *Energy Procedia* **2015**, *74*, 130–138. [[CrossRef](#)]
32. McQuiston, F.C.; Parker, J.D.; Spitler, J.D. *Heating, Ventilating, and Air Conditioning Analysis and Design*; John Wiley & Sons: Hoboken, NJ, USA, 2005; Volume 91.
33. Ying, Q.; Wang, H.; Lichtfouse, E. Numerical simulation on thermal behavior of partially filled metal foam composite phase change materials. *Appl. Therm. Eng.* **2023**, *229*, 120573. [[CrossRef](#)]
34. Alhusseney, A.; Al-Zurfi, N.; Nasser, A.; Al-Fatlawi, A.; Aljanabi, M. Impact of using a PCM-metal foam composite on charging/discharging process of bundled-tube LHTEs units. *Int. J. Heat Mass Transf.* **2020**, *150*, 119320. [[CrossRef](#)]

**Disclaimer/Publisher’s Note:** The statements, opinions and data contained in all publications are solely those of the individual author(s) and contributor(s) and not of MDPI and/or the editor(s). MDPI and/or the editor(s) disclaim responsibility for any injury to people or property resulting from any ideas, methods, instructions or products referred to in the content.